J Mol Neurosci (2012) 48:464–471
DOI 10.1007/s12031-012-9756-y

Demonstration of an Olfactory Bulb–Brain Translocation Pathway for ZnO Nanoparticles in Rodent Cells In Vitro and In Vivo

Yi-Yun Kao · Tsun-Jen Cheng · De-Ming Yang · Chin-Tien Wang · Yin-Mei Chiung · Pei-Shan Liu

Received: 29 December 2011 / Accepted: 16 March 2012 / Published online: 15 April 2012

Abstract ZnO nanoparticles (ZnO-NPs) are widely used in the engineering and cosmetic industries, and inhaled airborne particles pose a known hazard to human health; their translocation into humans is a recognized public health concern. The pulmonary–blood pathway for ZnO-NP toxicity is well documented, but whether translocation of these particles can also occur via an olfactory bulb–brain route remains unclear. The potential toxicity of ZnO-NPs for the human central nervous system (CNS) is predicated on the possibility of their translocation. Our study investigated translocation of ZnO-NPs both in vitro using the neuronal cell line PC12 and in vivo in a Sprague–Dawley rat model. Our findings indicate that the zinc-binding dye, Newport-Green DCF, binds ZnO stoichiometrically and that ZnO-NP concentration can therefore be measured by the fluorescence intensity of the bound dye in confocal fluorescence microscopy. Confocal data obtained using Newport-Green DCF-2 K^+-conjugated ZnO-NPs along with the membrane probe FM1-43 demonstrated endocytosis of ZnO-NPs by PC12 cells. In addition, Fluozin-3 measurement showed elevation of cytosolic Zn^{2+} concentration in these cells. Following in vivo nasal exposure of rats to airborne ZnO-NPs, olfactory bulbs and brains that were examined by Newport-Green fluorescence and TEM particle measurement clearly showed the presence of ZnO-NPs in brain. We conclude that an olfactory bulb–brain translocation pathway for airborne ZnO-NPs exists in rats, and that endocytosis is required for interneuron translocation of these particles.

Keywords Zinc oxide nanoparticles · Zn^{2+} · PC12 cells · Olfactory bulb–brain pathway

Abbreviation

ZnO-NPs	Zinc oxide nanoparticles
$[Zn^{2+}]_c$	Cytosolic Zn^{2+} concentration
NPG	Newport-Green
(NPG_s)	NPG salt form
CNS	Central nervous system

Y.-Y. Kao · P.-S. Liu (✉)
Department of Microbiology, Soochow University,
Shihlin, No. 70, Linxi Road, Shilin District,
Taipei 111, Taiwan
e-mail: psliu@mail.scu.edu.tw

T.-J. Cheng
Institute of Occupational Medicine and Industrial Hygiene,
College of Public Health, National Taiwan University,
Taipei, Taiwan

D.-M. Yang · C.-T. Wang
Department of Medical Research and Education,
Taipei Veterans General Hospital,
Taipei, Taiwan

D.-M. Yang
Institute of Biophotonics, National Yang-Ming University,
Taipei, Taiwan

C.-T. Wang
Institute of Clinical Medicine,
National Yang-Ming University School of Medicine,
Taipei, Taiwan

Y.-M. Chiung
Division of Medicine, Institute of Occupational Safety and Health,
Sijhih,
Taipei County, Taiwan

Y.-M. Chiung
Department of Microbiology and Immunology,
National Defense Medical Center,
Taipei, Taiwan

Introduction

The increasing use of zinc oxide nanoparticles (ZnO-NPs) in a number of important industries, such as semiconductor production and the manufacture of sunscreens (Greene et al. 2006), has brought attention to their potential health risks. Ailments caused by ZnO exposure have been extensively documented. In addition to pulmonary impairment and metal fume fever (Beckett et al. 2005), ZnO-NPs have been reported to cause apoptosis in neural stem cells (Deng et al. 2009), to interfere with ion channel currents in primary rat hippocampal neurons (Zhao et al. 2009), to induce morphological changes in rat brain tissue (Kozik et al. 1980), and to be involved in the pathogenesis of neuronal diseases (Frederickson et al. 2005). In an animal study, a Zn chelator was shown to reduce neuronal lesions, suggesting that high Zn levels were responsible for the central nervous system (CNS) damage (Cherny et al. 2001). A similar finding by Capasso et al. (2005) showed that high Zn levels could cause neuronal death. Because the concentration of airborne ZnO-NPs can be extremely high in welding factories and certain other industry workplaces, there is a potentially serious threat to CNS health if airborne ZnO-NPs can gain entry to the brain via an olfactory bulb–brain translocation pathway.

In contrast to problems posed by elevated Zn levels, Zn deficits in human patients and in mice have been implicated neurodegenerative disease, such as Parkinson's disease and Alzheimer's disease (AD) (Brewer et al. 2010). Serum zinc levels in AD patients were found to be significantly lower than controls (Baum et al. 2010), and in AD mice, zinc supplementation delayed hippocampus–dependent memory deficits and reduced β-amyloid accumulation (Corona et al. 2010). Thus, it appears that Zn homeostasis is critical for brain function and that either excessively high or low levels of Zn can interfere with normal neuronal function.

In an earlier study (Kao et al. 2012), we reported that ZnO-NP exposure elevated both cytosolic Zn^{2+} concentration ($[Zn^{2+}]_c$) and mitochondrial Zn^{2+} concentration ($[Zn^{2+}]_m$) in cultured cells as well as in rat white blood cells, via dissolution of ZnO in endosomes. The conversion of ZnO to ions after entry into cells has also been suggested by the study of Xia et al. (2008), which traced labeled ZnO, and showed that it disappeared in the lysosomes of BEAS-2B cells. Muller et al. (2010) showed that ZnO dissolved rapidly in a simulated body fluid having a lysosomal pH of 5.2, but that it is comparatively stable at the normal extracellular pH of 7.4. Thus, the existence of an olfactory bulb–brain entry pathway and potential for dissolution in endosomes would set the stage for ZnO-NPs to exert a profound effect upon zinc homeostasis, which plays a critical role in maintaining brain function.

Based on the finding that carbonaceous nanoparticles were detectable in the brain following nasal exposure (Oberdorster et al. 2004), it has been proposed that airborne particles deposited on the nasal olfactory epithelium may reach the brain by translocation along the olfactory nerve (Oberdorster et al. 2005). A number of studies have demonstrated that MnO_2 can make its way into brain via olfactory bulbs (Henriksson et al. 1999; Elder et al. 2006). Nevertheless, an olfactory bulb–brain pathway for ZnO-NP entry into the brain has not been established until now. In the brain, zinc levels are higher than those for manganese or other metals (Andrasi et al. 1995), which makes it difficult to detect an increase in Zn after ZnO-NP exposure, and it is also difficult to distinguish endogenous Zn from exogenous Zn coming from dissolution of ZnO. In the current study we describe a sensitive assay for ZnO-NPs in brain tissue and present evidence proving that the cellular process of endocytosis provides the link to translocate ZnO-NPs particles into neuron via an olfactory bulb–brain pathway.

Material and Methods

Materials

Sprague–Dawley (SD) rats were purchased from BioLASCO (Taipei, Taiwan). PC12cells were purchased from the research center BCRC 60048 (Hsinchu, Taiwan). SH-SY5Y cells were purchased from American Type Culture Collection. ZnO-NPs (<50 nm) were purchased from Sigma-Aldrich (St. Louis, MO, USA). Fluozin-3-AM, Newport-Green DCF-2 K^+, and FM 1-43 were purchased from Invitrogen (Grand Island, NY, USA). KCl, NaCl, and other salts were obtained from Merck KGaA (Darmstadt, German).

Cell Culture

PC12 cells were cultured in DMEM containing 5 % horse serum and 10 % fetal bovine serum on poly-L-lysine coated dishes or slides in 10 % CO_2, 37 °C (Liu and Chen 2010). SH-SY5Y cells were cultured in MEM medium containing 10 % FBS (Chiung et al. 2010).

ZnO-NP Preparation

ZnO-NPs (<50 nm) were freshly prepared by suspension and sonication in ultrapure water for 30 min (Branson 5510).

Scanning Electron Microscope (SEM)

ZnO-NP suspensions (0.8 mg/ml) were deposited and dried at room temperature. After sputter coating with platinum, samples were visualized by SEM (Nova™ NanoSEM 230).

Confocal Microscope Measurements

ZnO-NPs were labeled with Newport-Green DCF-2 K^+ (NPG_s, 10 μM) in ddH_2O with sonication. After 2 h incubation (with sonication), NPG_s-ZnO was collected by centrifugation at 10,000 rpm for 5 min. NPG_s-ZnO was freshly prepared before each experiment. PC12 cells were cultured on poly-L-lysine-coated glass slides and incubated with NPG_s-ZnO in the presence or absence of stimulants for 10 min in loading buffer. After incubation, slides were washed ten times in fresh loading buffer. For membrane visualization, cells were incubated simultaneously with 10 μM FM 1-43 for 10 min. Images were obtained with a confocal laser scanning microscope (CLSM; LSM 5 Pascal; Zeiss, Germany) with oil objectives (63×, NA 1.4; Zeiss, Germany). An argon 488 nm laser was used to excite NPG_s-ZnO. A He–Ne 543 nm laser was used to excite FM 1-43.

Cytosolic Free Zinc Concentration ($[Zn^{2+}]_c$) Measurements

Fluozin-3-AM was used to detect $[Zn^{2+}]_c$. Cells were loaded with 10 μM Fluozin-3-AM at 37 °C for 40 min and then washed three times for 30 min in loading buffer (150 mM NaCl, 5 mM KCl, 2.2 mM $CaCl_2$, 1 mM $MgCl_2$, 5 mM glucose, and 10 mM Hepes; pH 7.4). Fluorescence intensities were measured at an excitation wavelength of 494 nm and emission wavelength of 515 nm. R_{max} was achieved by adding excess zinc ion and digitonin to the cuvette at the end of the experiments; excess EGTA was subsequently added to obtain R_{min}. The relative $[Zn^{2+}]_c$ was normalized by dividing the net increase between R_{min} and R_{max}. For normalization, control cells were considered to be 100 %.

MTT Assay

Cells were seeded at 96 wells plates coated with poly-L-lysine. ZnO-NPs and $ZnCl_2$ were added 24 h after seeding. Cell viability was assessed using the colorimetric reagent, 3-[4,5-dimethylthiazol-2-yl]-2,5-diphenyl tetrazolium bromide (MTT) (Liu et al. 2011).

Trypan Blue

Cells were seeded in 6-well plates and treated with ZnO-NPs and $ZnCl_2$ for 24 h. The cells were harvested by trypsinization and counted in a hemocytometer after staining with Trypan blue (Park et al. 2006). The percentage cell death was expressed as the ratio of the number of Trypan blue-permeable cells to the total cell count.

ZnO-NP Generation and Rat Exposure

ZnO-NPs were generated by heating zinc powder to 570–600 °C in a ceramic crucible furnace. ZnO vapor was produced by reacting zinc vapor with oxygen in high-purity nitrogen gas. Before entering the major exposure chamber, ZnO vapors were mixed with filtered air in a series of cooling, humidifying, and diluting zones. The particle number, distribution and concentration were monitored by Scanning Mobility Particle Sizer and Condensation Particle Counter in the major exposure chamber. Eight-week-old male SD rats were used, following 1 week acclimatization to a 12-h light/dark cycle, 23±1 °C and 55±10 % humidity, and were randomly separated into two groups (consisting of six each), the HEPA control and ZnO-NP exposure group. Rats were housed in cages having a front tube connected to the major exposure chamber, either with (control group) or without (exposed group) HEPA air filters. Rats were sacrificed by barbital injection. Brains and olfactory bulbs were collected for measurements of ZnO-NPs. Our study was approved by the Institutional Animal Care and Use Committee at National Taiwan University.

Rat Olfactory Bulb Synaptosomes Preparation

Olfactory bulbs were collected from ZnO-NP-exposed and control SD rats (exposure conditions were 6 h for 1 day: 2.1×10^6 particles/cm^3; 38 nm particle size). Crude synaptosomes of each rat were prepared within 2 h at 2–4 °C following the method of Marcoli et al. (1999). Fluorescence intensities were measured at an excitation wavelength of 505 nm and emission wavelength of 535 nm.

Transmission Electron Microscope (TEM)

SD rats were exposed to ZnO-NPs (4 h on 3 consecutive days: 2.0×10^6, 3.4×10^6, and 6.6×10^6 particles/cm^3; 12–14 nm particle size). TEM samples were thin section cut through the rat left cerebrum which were fixed with 2.5 % glutaraldehyde, then 1 % osmium tetroxide in PBS (Maneta-Peyret et al. 1999). Sections were viewed by TEM (JEM 2000 EX-II) after staining with uranyl acetate and lead citrate.

Results

Newport-GreenDCF-2 K^+-Stained ZnO-NPs Reflects Fluorescence

NPG-DCF, a Zn^{2+}-sensitive dye (K_d=1 μM), has two forms, a cell-permeable ester (AM), and a membrane-impermeable water-soluble salt (2 K^+). We refer to the NPG-DCF-2 K^+ salt as NPG_s. We took advantage of our finding that ZnO-NPs can be labeled by NPG, but are not bound by Fluozin-3. The fluorescence image shows that NPG_s-ZnO-NPs are observable at 488 nm excitation; green laser (Fig. 1). No

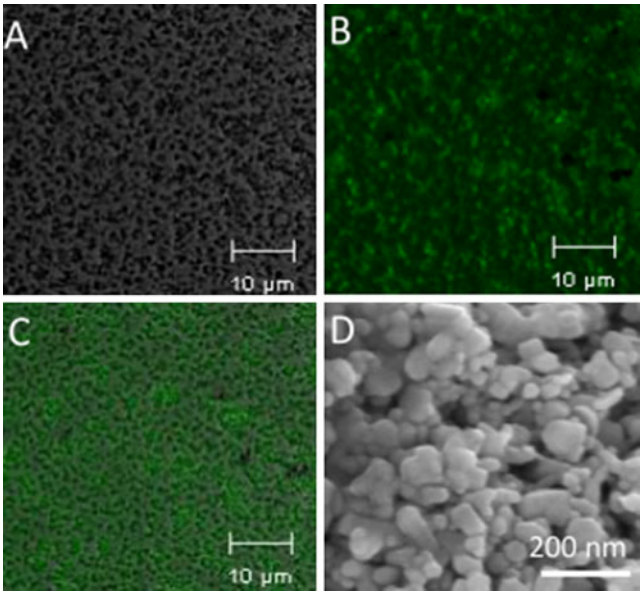

Fig. 1 Fluorescence of ZnO-NPs (<50 nm) stained with Newport-Green DCF-2 K^+. Stained particles were collected by washing and centrifugation. Confocal images of NPG_s-ZnO-NPs: **a** DIC, **b** green laser, and **c** merge, and **d** SEM image

fluorescence is seen following Fluozin-3 treatment of ZnO-NPs. SEM measurement was used to verify the size of NPG_s-ZnO-NPs. The average particle diameter was 40.4± 14.6 nm (Fig. 1d, n=30). We used the fluorescent and cell-impermeable character of NPG_s-ZnO-NPs in order to study their path of entry into cells. Instead of the membrane-permeable ester, the water-soluble NPG_s form of the dye was used to label the ZnO-NPs in order to prevent their direct diffusion across the plasma membrane.

Uptake of ZnO-NPs in Rat Pheochromocytoma PC12 Cells by Live Cell Confocal Imaging

NPG_s-ZnO-NPs were used to explore the fate of ZnO-NPs in PC12 cells. The PC12 cells were treated with 1 mM (81.4 μg/ml) NPG_s-ZnO-NPs in culture medium for 10 min. After ten washes in loading buffer, the NPG_s-ZnO-NP-treated PC12 cells were monitored at 488 nm excitation. In optical section images, ZnO-NPs were found to be intracellular (Fig. 2a). Some fluorescent spots appeared in the deeper optical sections but not in those taken at the cell surface, indicating an intracellular location. Since ATP stimulates the purinoceptor, P2, and evokes endocytosis following exocytosis in PC12 cells, we monitored cultured cells under these conditions. When treated with ATP and NPG_s-ZnO-NPs, more NPG_s-ZnO-NPs showed an intracellular location (Fig. 2b). To study the mechanism of ZnO-NP entry into the cells, we used NPG-ZnO together with FM1-43 in live-cell imaging. FM1-43 is a membrane probe widely used for monitoring recycling of vesicles (Hansen et al. 2009). Figure 2c shows that NPG_s-ZnO-NPs partially co-localized with FM1-43. Figure 2d shows that more vesicles appeared following ATP stimulation, and that NPG_s-ZnO-NPs co-localized with FM1-43, illustrating that most endocytic vesicles enclosed NPG_s-ZnO-NPs. We suggest that ZnO-NPs can enter neurons via endocytosis, and that P2 receptor stimulation enhances this endocytosis.

ZnO-NPs Induced an Increase in Free Zinc Ion Concentration ($[Zn^{2+}]_c$) in PC12 Cells

In addition, we investigated the conversion of ZnO-NPs to Zn^{2+} at the cellular level in our PC12 model. $[Zn^{2+}]_c$ was monitored in fluozin-3 experiments. Fluozin-3-AM-loaded PC12 cells were treated with ZnO-NPs and $[Zn^{2+}]_c$ was measured. Figure 3 shows that ZnO-NPs induced a rise in $[Zn^{2+}]_c$ in a dose- and time-dependent manner (within 60 min). $[Zn^{2+}]_c$ returned to resting levels within 24 h of exposure to ZnO-NPs at 8.1 and 81.4 μg/ml. However, cell viability decreased to 46.9±2.1 % of controls in cells receiving the higher dose (81.4 μg/ml for 24 h).

Similar Neurotoxicity Between ZnO-NPs and Zinc Ion

Neurotoxicity of ZnO-NPs was examined in rat PC12 and human SH-SY5Y cells. Figure 4 shows similar and significant neurotoxicity for both ZnO-NPs and Zn^2 at a concentration of 0.1 mM in PC12 cells and 1 mM in SH-SY5Y cells.

ZnO-NPs Were Found in Rat Olfactory Bulbs Following Exposure

An olfactory–brain translocation pathway has been proposed as the main route for NPs entering the brain (Oberdorster et al. 2005). In order to test this hypothesis for ZnO-NPs, Newport-Green DCF was used to measure total zinc concentration ([Zn]) in synaptosomes prepared from olfactory bulbs. Following exposure, synaptosome samples from exposed rats showed significantly higher [Zn] than those from HEPA control rats (p<0.1, Fig. 5a). This result supports the existence of olfactory–brain translocation as one probable route allowing ZnO-NPs to enter the brain following inhalation.

Existence of ZnO-NPs in Rat Brain After Exposure

We used TEM to investigate whether ZnO-NPs had entered the brains of exposed rats. Samples of ZnO-NP-exposed and control brains were compared. Figure 5b shows that sections from ZnO-NP-exposed rats exhibit numerous black spots which are rarely found in sections from HEPA-control rat brains. In endosomes, in particular, many small scars are present.

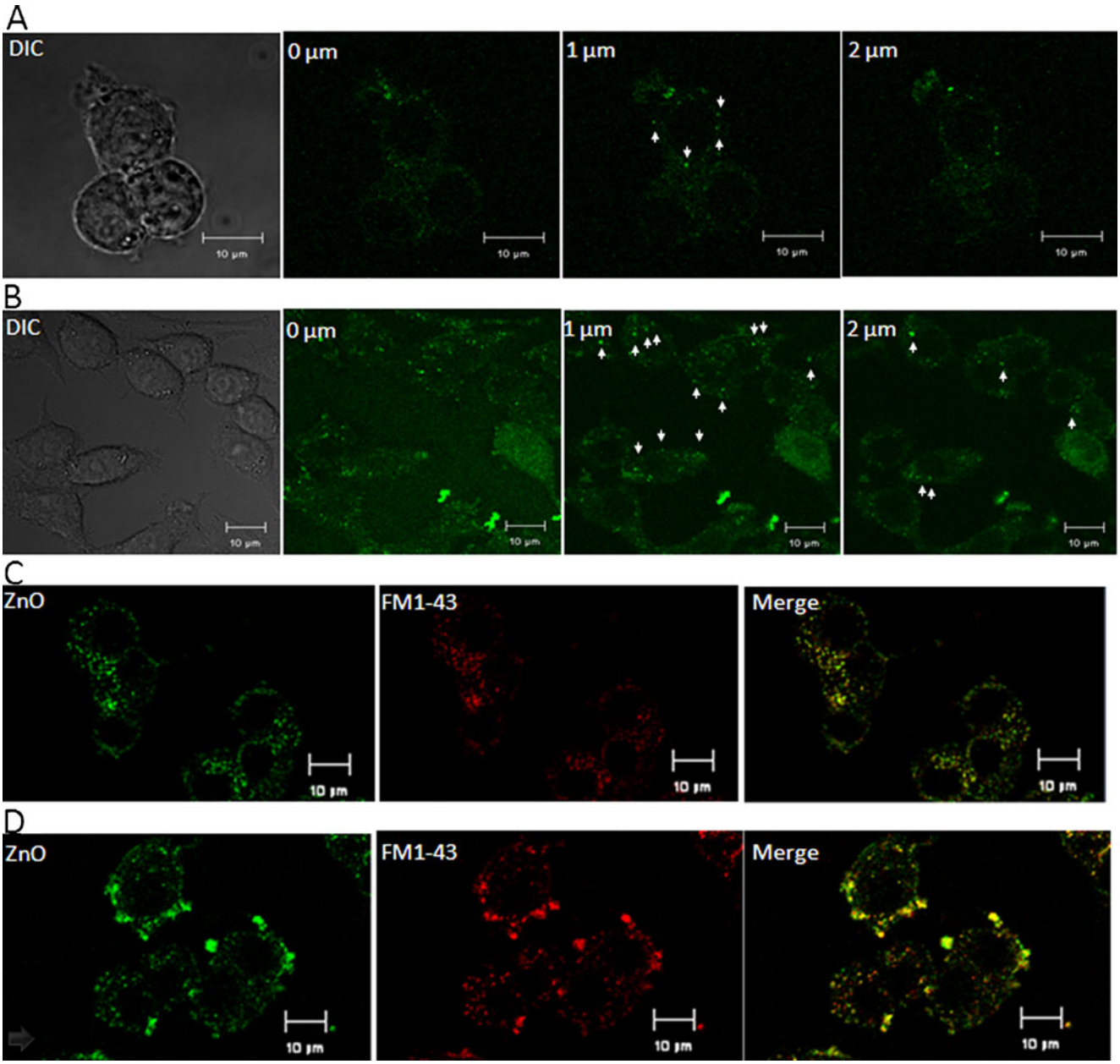

Fig. 2 Confocal images of PC12 cells treated with ZnO-NPs (<50 nm). Cells were treated with NPG_s-ZnO-NPs for 10 min, in either the absence (**a**) or presence (**b**) of 0.1 mM ATP. After washing, samples were observed and images obtained by confocal microscopy with cross-scan. *Arrows* indicate ZnO-NPs at sites within the cells that appear with increasing cross scan depth, and are not present in images taken at the cell surface. Cells treated with NPG_s-ZnO-NPs were stained with FM 1-43 for 10 min, in either the absence (**c**) or presence (**d**) of 0.1 mM ATP. Scale bar=10 µm. All observations were repeated five times on samples from different batches of cells. Representative images are shown

Discussion

The existence of a potential route for the entry of airborne ZnO-NPs into the CNS via an olfactory bulb–brain pathway is strongly supported by this study. Based on both our in vitro and in vivo data, we have outlined in detail some of the steps necessary to support an olfactory bulb–brain pathway for uptake of airborne ZnO-NPs: Step (1) involves translocation of ZnO-NPs occurs at olfactory bulbs first by endocytosis during inhalation. Data in Fig. 5a demonstrate the presence of ZnO-NPs in olfactory bulbs of exposed rats by Newport-Green Zn staining. In Fig. 2, endocytosis of NPG_s-ZnO-NPs by PC12 cells is shown in confocal fluorescence images. In Step (2), ZnO-NPs may be converted to Zn^{2+} in endosomes, and then be mobilized into the cytoplasm, leading to a rise in $[Zn^{2+}]_c$. An elevation in $[Zn^{2+}]_c$ following ZnO-NP exposure is measured in PC12 cells and data is shown in Fig. 3. In Step (3), ZnO-NPs and Zn^{2+} are

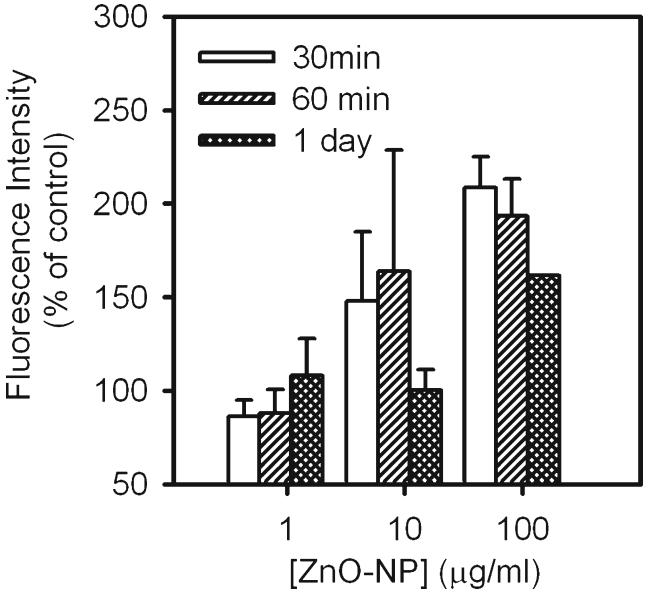

Fig. 3 The changes of $[Zn^{2+}]_c$ in PC12 cells. The $[Zn^{2+}]_c$ was measured in fluozin-3-AM-loaded PC12 cells pretreated with ZnO-NPs (<50 nm) at various concentrations for times shown. Data are mean ± SE from three separate batches of cells. The fluorescence intensity of control PC12 cells (no ZnO-NP treatment) was set as 100 %, and used to normalize experimental results

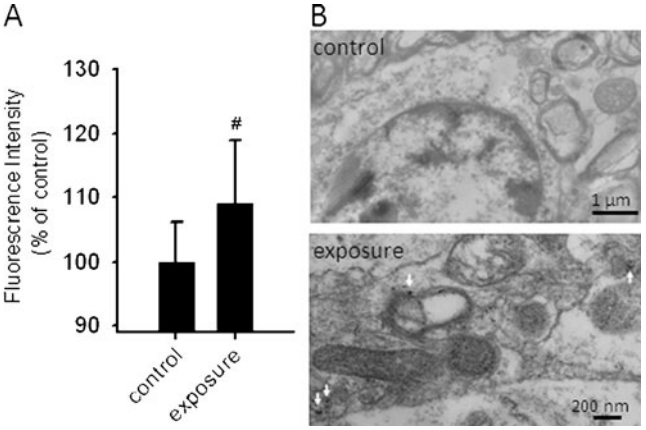

Fig. 5 The existence of ZnO-NPs in SD rat olfactory bulbs and brains. **a** Olfactory bulb synaptosomes were isolated from ZnO-NP-exposed rats and from HEPA control animals, and were loaded with 10 μM Newport-Green DCF (AM form). Fluorescence measurements were carried out at an excitation wavelength of 505 nm and emission wavelength of 535 nm. Data represent mean ± SE from six rats. The mean values of control samples were treated as 100 %. #$p<0.1$. **b** Transmission electron micrograph images of rat brain slice after ZnO-NP exposure. Magnifications are ×18,000 and ×50,000 for HEPA-control and ZnO-NP-exposed brain images, respectively. White arrows indicate ZnO-NPs (electron-dense black spots). All observations were repeated three times using different batches of rats, six animals each for the experimental (exposed) and control (non-exposed) groups, in each batch

translocated from the olfactory sensory neuron to the signal-processing neuron through the gap junction or by exocytosis in the presynaptic neuron followed by endocytosis in the postsynaptic neuron, thus reaching the CNS. The presence of ZnO-NPs in rat brain tissue is shown in our TEM images. All steps documented here support the olfactory bulb–brain translocation of ZnO-NPs.

The olfactory bulb–brain pathway is proposed as a portal of entry to the CNS under conditions of exposure to small sized particles. An olfactory translocation route was described as early as the 1940s, for 30 nm polio virus that had been introduced intranasally into chimpanzees and rhesus monkeys (Howe and Bodian 1941). The olfactory bulb–brain translocation pathway was proposed (Oberdorster et al. 2005) and given support in the instance of MnO (Elder et al. 2006); however, Ghio and Bennett (2007) presented data disputing the likelihood of this route for entrance into CNS. In addition to ZnO-NPs, silver-coated colloidal gold particles (50 nm), manganese, cadmium, nickel, and inorganic mercury all have been reported to be transported via the

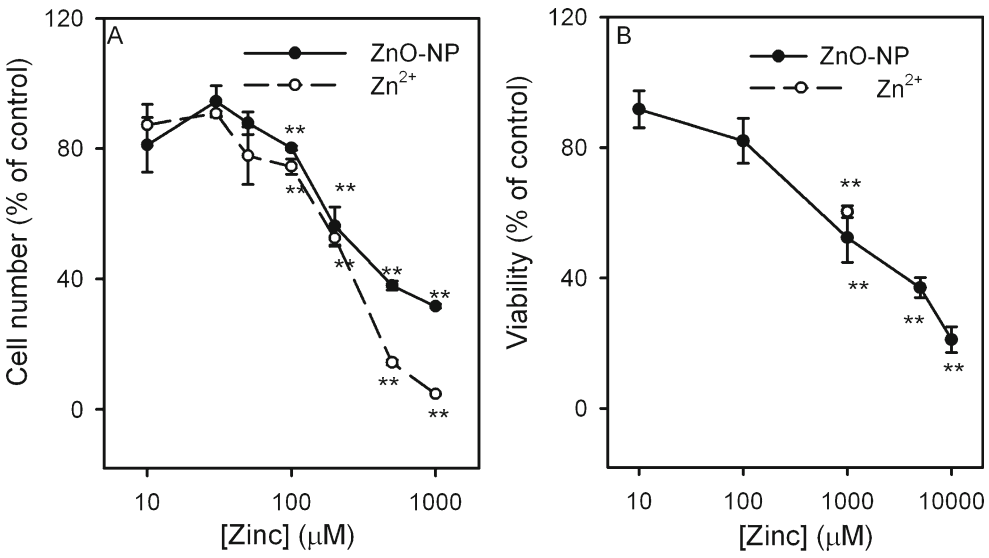

Fig. 4 Effects of Zinc ions and ZnO-NPs on cytoviability in rat pheochromocytoma PC12 cells and human neuroblastoma SH-SY5Y cells. Panel A, PC12 cells were treated with ZnO-NPs and ZnCl solution at various concentrations for 24 h, and viability was determined by MTT. Panel B, SH-SY5Y cells were treated with various concentrations of ZnO-NPs or ZnCl solution for 24 h, and viability determined by Trypan blue staining. The data are expressed as mean ± SD. *$p<0.05$; **$p<0.01$

olfactory bulb (De Lorenzo 1957; Tjalve et al. 1996; Henriksson et al. 1997; Henriksson and Tjalve 1998). With regard to the size of NPs, our study is the first to demonstrate that airborne ZnO-NPs can enter the CNS of mammals via an olfactory bulb–brain translocation pathway.

A number of laboratories have shown that NPs can be engulfed during endocytosis in both excitable and non-excitable cells. In the rat model, stimulation by ozone, hydrogen peroxide, or histamine increases the permeability of lung epithelial and endothelial barriers to NPs (192Ir-UFP aerosol) (Meiring et al. 2005). Magnetic nanoparticles have been shown to be internalized into A549 lung epithelial cells via an energy-dependent endosomal-lysosomal mechanism (Kim et al. 2006), and transferrin-mediated uptake of gold nanoparticles by human nasopharyngeal carcinoma cells by human nasopharyngeal carcinoma cells has been shown (Yang et al. 2005). Our data establish that NPG_s-ZnO-NPs are endocytosed by PC12 cells, and that this endocytosis is enhanced by stimulation of the P2-purinoceptor by ATP. Because the mean diameter of the P2X7 channel is less than 0.85 nm (Riedel et al. 2007), much smaller than the size of most ZnO-NPs, we rule out the possibility that dye–ZnO-NPs complexes can influx into cells via the P2 channel.

Zinc is critical for the growth and survival of neurons, yet high levels of zinc are cytotoxic. Our study shows that both zinc ions and ZnO-NPs above 0.1 mM are cytotoxic. An elevation in $[Zn^{2+}]_c$ could be caused by an increase as little as 1 μg/ml (12 μM). Therefore, it is possible for $[Zn^{2+}]_c$ to be elevated by non-toxic ZnO concentrations. The olfactory bulb–brain translocation route provides a pathway explaining ZnO can enter the CNS and achieve an elevation $[Zn^{2+}]_c$ without causing cell damage.

Zinc homeostasis is critical to neuronal health. Zinc modulates the structure of proteins at postsynaptic sites to maintain neuronal functions (Gundelfinger et al. 2006). This study shows that ZnO-NP exposure followed by endocytosis can interfere with zinc homeostasis, a finding that is supported by our previous work (Kao et al. 2012). In that study, we demonstrated that dissolution of ZnO-NPs to zinc ions could occur at the low pH of endosomes (pH 5.5), allowing Zn^{2+} to then leak into the cytosol. Similar dissolution may occur in the endosome of PC12 cells following engulfment of ZnO-NPs. We suggest that ZnO-NPs first enter cells via endocytosis and are then converted to Zn^{2+} in endosomes, leading to an elevation of $[Zn^{2+}]_c$. Moreover, our observation that $[Zn^{2+}]_c$ in cells exposed to ZnO-NPs for 24 h returned to basal levels, and that nearly half of exposed cells died following exposure to high concentration of ZnO-NPs**.** We suggest that the surviving cells under these conditions retained their capability for zinc homeostasis, as evidenced by their return to basal $[Zn^{2+}]_c$ levels, while death of a subpopulation of cells was caused by extreme changes in their $[Zn^{2+}]_c$, exceeding their capacity for maintaining homeostasis. The fact that $[Zn^{2+}]_c$ of surviving cells following 24 h ZnO-NP exposure returned to basal levels, suggests that homeostasis of $[Zn^{2+}]_c$ is vital to cell survival.

In this study, exposure to ZnO-NPs significantly increased zinc levels in the olfactory bulb (Fig. 5). In brain, starting zinc levels are high, making it difficult to accurately measure changes following ZnO-NP exposure. According to a report by Andrasi et al. (1995), zinc levels in the normal human brain were 15- to 73-fold higher than manganese, and 24- to 51-fold higher than aluminum. Zinc concentrations are also known to vary in different regions of the brain, (47–102 μg/g, wt) and show a large variation among individuals (n=20) in the same regions in normal human brain (40 % variation in cortex centralis). Accordingly, our ICP-MS measurements of total zinc in brain tissue were almost identical for exposed and HEPA control rats (data not shown). TEM images shown in Fig. 5 also demonstrate the existence of ZnO-NPs in brain tissue following ZnO-NP exposure. We conclude that this study showed both in vitro and in vivo evidence of airborne ZnO-NPs entering the CNS via an olfactory bulb–brain translocation pathway.

Acknowledgements We thank all members of the ZnO-NP team, supported by the National Science Council, especially Miss Jung-Yen Liu, Meng Ho, and Miao-Chuan Yu for expert assistance with animal care and dissection. We also deeply appreciate Ms Suzanne Hosier's critical editing of the English text. This work was supported by grants from the National Science Council, Taiwan, R.O.C. (NSC-96-2621-Z-031-001, NSC-97-2320-B-031-001 and NSC-97-2320-B-031-001) and Institute of Occupational Safety and Health, Taiwan, ROC (IOSH101-M326).

References

Andrasi E, Farkas E, Scheibler H, Reffy A, Bezur L (1995) Al, Zn, Cu, Mn and Fe levels in brain in Alzheimer's disease. Arch Gerontol Geriatr 21:89–97

Baum L, Chan IH, Cheung SK, Goggins WB, Mok V, Lam L, Leung V, Hui E, Ng C, Woo J, Chiu HF, Zee BC, Cheng W, Chan MH, Szeto S, Lui V, Tsoh J, Bush AI, Lam CW, Kwok T (2010) Serum zinc is decreased in Alzheimer's disease and serum arsenic correlates positively with cognitive ability. Biometals 23:173–179

Beckett WS, Chalupa DF, Pauly-Brown A, Speers DM, Stewart JC, Frampton MW, Utell MJ, Huang LS, Cox C, Zareba W, Oberdorster G (2005) Comparing inhaled ultrafine versus fine zinc oxide particles in healthy adults: a human inhalation study. Am J Respir Crit Care Med 171:1129–1135

Brewer GJ, Kanzer SH, Zimmerman EA, Molho ES, Celmins DF, Heckman SM, Dick R (2010) Subclinical zinc deficiency in Alzheimer's disease and Parkinson's disease. Am J Alzheimers Dis Other Demen 25:572–575

Capasso M, Jeng JM, Malavolta M, Mocchegiani E, Sensi SL (2005) Zinc dyshomeostasis: a key modulator of neuronal injury. J Alzheimers Dis 8:93–108, discussion 209–115

Cherny RA, Atwood CS, Xilinas ME, Gray DN, Jones WD, McLean CA, Barnham KJ, Volitakis I, Fraser FW, Kim Y, Huang X, Goldstein LE, Moir RD, Lim JT, Beyreuther K, Zheng H, Tanzi

RE, Masters CL, Bush AI (2001) Treatment with a copper–zinc chelator markedly and rapidly inhibits beta-amyloid accumulation in Alzheimer's disease transgenic mice. Neuron 30:665–676

Chiung YM, Kao YY, Chang WF, Yao CW, Liu PS (2010) Toluene diisocyanate (TDI) induces calcium elevation and interleukine-4 (IL-4) release — early responses upon TDI stimulation. J Toxicol Sci 35:197–207

Corona C, Masciopinto F, Silvestri E, Viscovo AD, Lattanzio R, Sorda RL, Ciavardelli D, Goglia F, Piantelli M, Canzoniero LM, Sensi SL (2010) Dietary zinc supplementation of 3xTg-AD mice increases BDNF levels and prevents cognitive deficits as well as mitochondrial dysfunction. Cell Death Dis 1:e91

De Lorenzo AJ (1957) Electron microscopic observations of the olfactory mucosa and olfactory nerve. J Biophys Biochem Cytol 3:839–850

Deng X, Luan Q, Chen W, Wang Y, Wu M, Zhang H, Jiao Z (2009) Nanosized zinc oxide particles induce neural stem cell apoptosis. Nanotechnology 20:115101

Elder A, Gelein R, Silva V, Feikert T, Opanashuk L, Carter J, Potter R, Maynard A, Ito Y, Finkelstein J, Oberdorster G (2006) Translocation of inhaled ultrafine manganese oxide particles to the central nervous system. Environ Health Perspect 114:1172–1178

Frederickson CJ, Koh JY, Bush AI (2005) The neurobiology of zinc in health and disease. Nat Rev Neurosci 6:449–462

Ghio AJ, Bennett WD (2007) Metal particles are inappropriate for testing a postulate of extrapulmonary transport. Environ Health Perspect 115:A70, author reply A70–A71

Greene LE, Yuhas BD, Law M, Zitoun D, Yang P (2006) Solution-grown zinc oxide nanowires. Inorg Chem 45:7535–7543

Gundelfinger ED, Boeckers TM, Baron MK, Bowie JU (2006) A role for zinc in postsynaptic density asSAMbly and plasticity. Trends Biochem Sci 31:366–373

Hansen GH, Rasmussen K, Niels-Christiansen LL, Danielsen EM (2009) Endocytic trafficking from the small intestinal brush border probed with FM dye. Am J Physiol Gastrointest Liver Physiol 297:G708–G715

Henriksson J, Tjalve H (1998) Uptake of inorganic mercury in the olfactory bulbs via olfactory pathways in rats. Environ Res 77:130–140

Henriksson J, Tallkvist J, Tjalve H (1997) Uptake of nickel into the brain via olfactory neurons in rats. Toxicol Lett 91:153–162

Henriksson J, Tallkvist J, Tjalve H (1999) Transport of manganese via the olfactory pathway in rats: dosage dependency of the uptake and subcellular distribution of the metal in the olfactory epithelium and the brain. Toxicol Appl Pharmacol 156:119–128

Howe HA, Bodian D (1941) Second attacks of poliomyelitis: an experimental study. J Exp Med 74:145–166

Kao YY, Chen YC, Cheng TJ, Chiung YM, Liu PS (2012) Zinc oxide nanoparticles interfere with zinc ion homeostasis to cause cytotoxicity. Toxicol Sci 125:462–472

Kim JS, Yoon TJ, Yu KN, Noh MS, Woo M, Kim BG, Lee KH, Sohn BH, Park SB, Lee JK, Cho MH (2006) Cellular uptake of magnetic nanoparticle is mediated through energy-dependent endocytosis in A549 cells. J Vet Sci 7:321–326

Kozik MB, Maziarz L, Godlewski A (1980) Morphological and histochemical changes occurring in the brain of rats fed large doses of zinc oxide. Folia Histochem Cytochem (Krakow) 18:201–206

Liu PS, Chen CY (2010) Butyl benzyl phthalate suppresses the ATP-induced cell proliferation in human osteosarcoma HOS cells. Toxicol Appl Pharmacol 244(3):308–314

Liu PS, Chen YY, Feng CK, Lin YH, Yu TC (2011) Muscarinic acetylcholine receptors present in human osteoblast and bone tissue. Eur J Pharmacol 650:34–40

Maneta-Peyret L, Compere P, Moreau P, Goffinet G, Cassagne C (1999) Immunocytochemistry of lipids: chemical fixatives have dramatic effects on the preservation of tissue lipids. Histochem J 31:541–547

Marcoli M, Maura G, Munari C, Ruelle A, Raiteri M (1999) Pharmacological diversity between native human 5-HT1B and 5-HT1D receptors sited on different neurons and involved in different functions. Br J Pharmacol 126:607–612

Meiring JJ, Borm PJ, Bagate K, Semmler M, Seitz J, Takenaka S, Kreyling WG (2005) The influence of hydrogen peroxide and histamine on lung permeability and translocation of iridium nanoparticles in the isolated perfused rat lung. Part Fibre Toxicol 2:3

Muller KH, Kulkarni J, Motskin M, Goode A, Winship P, Skepper JN, Ryan MP, Porter AE (2010) pH-dependent toxicity of high aspect ratio ZnO nanowires in macrophages due to intracellular dissolution. ACS Nano 4:6767–6779

Oberdorster G, Sharp Z, Atudorei V, Elder A, Gelein R, Kreyling W, Cox C (2004) Translocation of inhaled ultrafine particles to the brain. Inhal Toxicol 16:437–445

Oberdorster G, Oberdorster E, Oberdorster J (2005) Nanotoxicology: an emerging discipline evolving from studies of ultrafine particles. Environ Health Perspect 113:823–839

Park YP, Choi SC, Cho MY, Song EY, Kim JW, Paik SG, Kim YK, Lee HG (2006) Modulation of telomerase activity and human telomerase reverse transcriptase expression by caspases and bcl-2 family proteins in Cisplatin-induced cell death. Korean J Lab Med 26:287–293

Riedel T, Schmalzing G, Markwardt F (2007) Influence of extracellular monovalent cations on pore and gating properties of P2X7 receptor-operated single-channel currents. Biophys J 93:846–858

Tjalve H, Henriksson J, Tallkvist J, Larsson BS, Lindquist NG (1996) Uptake of manganese and cadmium from the nasal mucosa into the central nervous system via olfactory pathways in rats. Pharmacol Toxicol 79:347–356

Xia T, Kovochich M, Liong M, Madler L, Gilbert B, Shi H, Yeh JI, Zink JI, Nel AE (2008) Comparison of the mechanism of toxicity of zinc oxide and cerium oxide nanoparticles based on dissolution and oxidative stress properties. ACS Nano 2:2121–2134

Yang PH, Sun X, Chiu JF, Sun H, He QY (2005) Transferrin-mediated gold nanoparticle cellular uptake. Bioconjug Chem 16:494–496

Zhao J, Xu L, Zhang T, Ren G, Yang Z (2009) Influences of nanoparticle zinc oxide on acutely isolated rat hippocampal CA3 pyramidal neurons. Neurotoxicology 30:220–230